Correlation between spectra and structural data of YAG:Tm^{3+} and YAG:Cr^{3+}, Tm^{3+}

A. Lupei, C. Tiseanu, and V. Lupei
Institute of Atomic Physics, Bucharest 76900, Romania
(Received 16 July 1992; revised manuscript received 16 December 1992)

In order to elucidate the Stark structure of Tm^{3+} multiplets involved in the ≈ 2 μm emission of YAG:Tm^{3+}, and YAG:Cr^{3+},Tm^{3+}, absorption and emission spectra have been measured over a wide range of concentrations. The Tm^{3+} spectra in YAG show, besides the main lines assigned to dodecahedral D_2 sites, a set of satellites associated with Tm^{3+} in perturbed sites. An attempt to correlate Tm^{3+} spectra with YAG structure and structural defects has been made. Using our data and an improved algorithm we have been able to identify Stark levels of Tm^{3+} in D_2 (Y^{3+}) sites, especially in the $^3F_4$, $^3H_4$, $^3F_3$, and $^3F_2$ multiplets. The spectra due to Tm^{3+} in perturbed sites, with a lower symmetry, were used to assign levels corresponding to forbidden transitions in the D_2 symmetry. Some of the identified levels in $^3H_4$ can explain the luminescence data and the cross-relaxation mechanism that lead to the population of the $^3F_4$ metastable level, while those in $^3F_3$ seem to play an important role in Cr^{3+}-Tm^{3+} energy transfer. In Cr^{3+}-codoped samples supplementary lines in both Cr^{3+} and Tm^{3+} spectra as well as a preferential energy transfer have been observed and explained in terms of structural data.

I. INTRODUCTION

Solid-state laser systems for emission in the 2 μm range are of great practical interest. Among the systems investigated in recent years, YAG:Tm^{3+} and YAG:Cr^{3+}, Tm^{3+} proved to be particularly successful.[1–3] In both systems, at high Tm^{3+} content, energy transfer processes are important for laser emission. The 2 μm emission of YAG:Tm^{3+} or YAG:Cr, Tm^{3+} is generated by a transition between the $^3F_4$ and $^3H_6$ Tm^{3+} levels (Fig. 1) while the main states involved in excitation (under xenon lamp pumping) span the energy range up to $\approx {}^3F_2$. From the $^3F_2$ and $^3F_3$ pumping levels the excitation goes nonradiatively to $^3H_4$ which, in turn, populates the $^3F_4$ metastable level by a cross-relaxation process. In the Cr^{3+}-codoped crystals an enhancement of population in $^3F_2$ and $^3F_3$ levels by Cr^{3+}-Tm^{3+} transfer is assumed. In addition to luminescence kinetics measurements, a correct interpretation of these processes requires a detailed energy level diagram for Tm^{3+} in YAG as well as an understanding of the possible spectral modifications in the concentrated or in doubly doped samples. Until recently[4] relatively little information could be found on the spectra of YAG:Tm^{3+} (Refs. 5 and 6) or YAG:Cr^{3+},Tm^{3+}.[7,8] The detailed investigations performed by Gruber *et al.*[4] on YAG:Tm^{3+} spectra indicated that Tm^{3+} ions preferentially occupy dodecahedral D_2 (Y^{3+}) positions, although several weak satellites attributed to perturbed sites were noticed. The most intense lines were analyzed using the selection rules for the D_2 symmetry, while the others, weak to moderately strong peaks whose relatively intensity was independent on Tm content, were only reported.

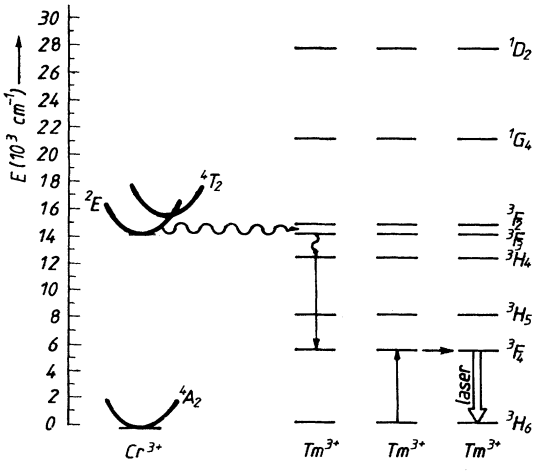

FIG. 1. Energy level diagram of Tm^{3+} and Cr^{3+} in YAG and main processes involved in ≈ 2 μm emission.

The major problem in the analysis of $Tm^{3+}(4f^{12})$ non-Kramers ion spectra lies in the difficulty of identifying the symmetry of Stark levels in a cubic crystal (the overall symmetry of garnets) without polarization measurements. To overcome this difficulty a combination of experimental data and crystal-field calculation was used.[4]

By using a lattice sum calculation that included point charge, dipole-dipole, and self-induced contributions, the fundamental Stark level of the Tm^{3+} ground multiplet $^3H_6$ was established as Γ_2. The assignment of other Stark levels is based on an algorithm that uses the positions of hot bands in absorption and laser excited luminescence lines from specific Stark levels. This assignment is then compared with the results from crystal-field splitting calculations.

There are several difficulties in such an analysis that must be stressed: (i) the known shortcomings of a crystal-field calculation, especially when one has to work with such a large number of parameters (nine besides the free-ion ones in this case); (ii) the possibility of low intensity or missing lines corresponding to allowed transitions; (iii) the superposition of high-energy Stark levels in some

multiplets with phonon sidebands.

In our investigation of the nature of luminescence quenching of Tm^{3+} in YAG, differences have been noticed in the spectra as compared with those reported in Ref. 4. For this reason the absorption and emission spectra of Tm^{3+} in YAG crystals have been systematically investigated over a wide range of concentrations with special attention to the levels involved in the ≈ 2 μm emission. Differences have been noticed mainly in the hot band positions in some regions (better resolved in our samples, with Tm^{3+} up to ≈ 5 at. %), as well as multisite structure and luminescence spectra. The low-temperature absorption spectra and the assignment procedure of Gruber *et al.*[4] has been of great help and we shall also use their notation.

Assuming that the symmetry of the ground level is Γ_2 as determined in Ref. 4, an improved algorithm has been used to assign the excited Stark levels. This procedure was based on a convention in the selection of the local axes of a D_2 group [similar to that used in the site-selective polarized spectroscopy of Tb^{3+} in YAG (Ref. 10)], and on the use of a multisite structure to locate excited Γ_2 levels corresponding to transitions from the ground level that are forbidden in the D_2 symmetry. The modifications of static Tm^{3+} and Cr^{3+} spectra in doubly doped YAG crystals are also presented and the importance of multisite structure in the investigation of $Tm^3 \rightarrow Tm^{3+}$ or $Cr^{3+} \rightarrow Tm^{3+}$ energy transfer is discussed.

II. STRUCTURAL CONSIDERATIONS

The YAG crystal has cubic O_h^{10} symmetry, and the crystallographic unit cell contains eight $Y_3Al_5O_{12}$ chemical units.[11] All 24 Y^{3+} ions occupy dodecahedral c sites of D_2 symmetry; 16 of the Al^{3+} ions occupy octahedral a sites of C_{3i} symmetry and the remaining 24 Al^{3+} ions are tetrahedrally coordinated by oxygens, in d sites of S_4 symmetry. Trivalent rare-earth ions are usually substituted for Y^{3+} in c sites (although minority octahedral sites could be occupied by small ions), while Cr^{3+} ions are substituted for Al^{3+} only in octahedral a-sites.

$Tm^{3+}(4f^{12})$ is a non-Kramers ion whose spectral properties in the normal c sites are described by the D_2 point group. The D_2 group has four one-dimensional irreducible representations Γ_i ($i=1-4$) and each J multiplet of Tm^{3+} is split into $2J+1$ singlet Stark components. The selection rules for electric dipole (P_i) and magnetic dipole (M_i) transitions are given in Table I, where x, y, and z are the local axes of D_2. One of the D_2 axes lies along the cubic unit-cell edge, while the other two are directed along face diagonals.

The data on YAG show that the local symmetry at the Tm^{3+} (c) site is D_2 as a slight perturbation of a higher symmetry environment D_{2d}, in which the fourfold axis has been reduced to one of the axes parallel to face diagonals. Thus, we follow the same convention for the local axes of D_2 that was used in the case of site-selective polarized spectroscopy of Tb^{3+} in YAG:[10] the x axis parallel with cubic cell axes and the z axis corresponding to the fourfold axis of D_{2d}.

TABLE I. Electric- and magnetic-dipole selection rules for the D_2 group.

	Γ_1	Γ_2	Γ_3	Γ_4
Γ_1		$P_y(M_y)$	$P_z(M_z)$	$P_x(M_x)$
Γ_2	$P_y(M_y)$		$P_x(M_x)$	$P_z(M_z)$
Γ_3	$P_z(M_z)$	$P_x(M_x)$		$P_y(M_y)$
Γ_4	$P_x(M_x)$	$P_z(M_z)$	$P_y(M_y)$	

For isolated Tm^{3+} ions in c sites (D_2 symmetry) the $\Gamma_i \rightarrow \Gamma_i$ transitions are forbidden as either electric or magnetic dipoles. However, the true local symmetry at Tm^{3+} normal sites could be lower. Even in the purest YAG crystals there are known at least two such sources of symmetry lowering:[2] (i) the presence of other Tm^{3+} ions in the nearest-neighbor c sites and (ii) the departure from stoichiometry (larger Y^{3+} content) in the high-temperature (melt) grown YAG crystals. These perturbations of the crystal field can lead to shifts of Stark components and the appearance of satellite lines.

Due to random occupation of cationic sites, nearest-neighbor $Tm^{3+}(c)-Tm^{3+}(c)$ pairs can occur even at very low concentrations. Since in YAG every c site is surrounded by four other c sites forming a tetrahedron, one would expect only one satellite, labeled by M,[12] due to the nearest-neighbor pairs, with relative intensity increasing linearly with concentration. At high Tm^{3+} content, besides pairs, complex formations of three or more ions can appear.

A common stoichiometric deviation in the melt-grown YAG crystals is the occupation of part (1.5–2 %) of the octahedral Al^{3+} sites by Y^{3+} ions.[12] Such a defect Y^{3+} (a) site is surrounded by a first coordination sphere of six c sites spaced at a distance of 3.35 Å and a second sphere of six sites at 5.4 Å. In both cases the octahedra of c sites are distorted but preserve the inversion. The central Y^{3+} (a) site could produce three different perturbations in the first sphere of c sites and three other much weaker perturbations in the second sphere. These perturbations lead to satellite lines—labeled by P.[12] The number of resolved P satellites depends on the particular ion and transition.[12,13] The P satellites due to a Y^{3+} (a) defect can be distinguished from other satellites since the relative intensity is independent of activator concentration. Codoping the crystals with Cr^{3+} ions, which occupy only a sites, can produce new perturbations at Tm^{3+} (c) sites, similar to those caused by a defect Y^{3+} (a), but the intensities of such satellites are expected to depend linearly on Cr^{3+} concentration. Perturbing effects could be expected in the Cr^{3+} (a) spectra that have an adjacent Tm^{3+} (c). One should mention that Tm^{3+} can also substitute into octahedral Al^{3+} a sites giving rise to a competition in the occupation of a sites by an excess of Y^{3+} or Cr^{3+} and Tm^{3+} ions.

Regardless of whether the perturbing effect on Tm^{3+} (c) is due to another adjacent c-Tm^{3+} or to Y^{3+} and Cr^{3+} ions in a sites, the local symmetry is reduced from D_2. In any subgroup of D_2 all the transitions between Stark levels of various J multiplets are electric-dipole allowed;

thus, the forbidden $\Gamma_i \rightarrow \Gamma_i$ transitions in D_2 become allowed and satellite structure can appear even if the main lines of Tm^{3+} (*c*) are absent. The intensity of such lines depends on the strength of the perturbation.

The Tm^{3+} spectra in YAG could also be complicated due to the Tm^{3+} ions in octahedral *a* sites. Since such a site has trigonal symmetry with inversion, the electric-dipole transitions are forbidden and magnetic-dipole transitions can connect only levels with $\Delta J = \pm 1$.[12] However, due to crystal-field J mixing, many more transitions could be expected, although their intensity would be weak.

These structural and group-theoretical arguments shall be used in the identification of Tm^{3+} spectra in YAG and in an attempt to assign symmetry labels to Tm^{3+} Stark levels. We shall use the algorithm proposed earlier with an improvement concerning the identification of excited Γ_2 levels whose transitions from the ground state would be forbidden in D_2 symmetry. One can expect to find Γ_2 levels in absorption regions where *P*-type satellites are present, without noticeable main lines. Using this supplementary argument we have identified several Γ_2 levels, clearly verified from luminescence data.

Since the D_2 local symmetry at Tm^{3+} (*c*) sites can be considered as a slight distortion of D_{2d}, one would expect to have intense lines that are compatible with the electric-dipole-allowed transitions in D_{2d} as well. For example, the $\Gamma_2 \leftrightarrow \Gamma_4$ P_z transitions in D_2 correspond to an electric-dipole allowed transition in D_{2d} ($\Gamma_5 \leftrightarrow \Gamma_5$). But following the arguments given in Ref. 9, the same group-theory-allowed transitions in D_2 can also correspond to transitions forbidden according to D_{2d} selection rules, since the same notation in D_2 corresponds to two levels in D_{2d}. Thus, one could explain low intensity or missing lines of the spectra (e.g., $\Gamma_1 \leftrightarrow \Gamma_3$).

III. EXPERIMENT

Samples of YAG:Tm^{3+} with concentrations varying between 0.1 and ≈ 6 at. %, and YAG:Cr^{3+},Tm^{3+} with Cr^{3+} content between ≈ 0.1 and ≈ 1 at. % and Tm^{3+} content from ≈ 1 to ≈ 5 at. % were obtained by the Czochralski method. Absorption and emission measurements were performed at 77 K and at higher temperatures with a Cary 17 spectrometer. The visible region was also measured at higher resolution (≈ 0.1 Å) at 10 K using for detection a phase-sensitive system. The luminescence excited with the second and third harmonics of a YAG:Nd^{3+} laser and detected with a boxcar integrator PAR 162 was also analyzed.

IV. SPECTRA

A. YAG:Tm^{3+} transmission spectra

Transmission spectra of Tm^{3+} in YAG, for each J multiplet, include several sharp intense peaks, a series of hot bands (temperature-dependent lines that in some cases are very intense), and a number of small peaks (especially in high-resolution spectra). A characteristic of the spectra is that, for each multiplet, the lines are broadened at higher energies due to phonon interaction. Some phonon sidebands can also appear and the identification of Stark components is difficult.

Generally, the transmission spectra show many similarities with those reported in Table III of Ref. 4. Thus, the positions of most of the main lines and satellite lines are in agreement. Differences have been noticed in hot band structure in some regions and the presence of several supplementary lines. Thus, the temperature dependence in many spectral regions give the positions of some Z_i Stark components of the $^3H_6$ multiplet: Z_2 at 27 cm^{-1}, Z_3 at 215 cm^{-1}, Z_4 at 240 cm^{-1}, Z_5 at 247 cm^{-1} as in Ref. 4.

Few differences have been noticed in the hot band structure of the $^3H_6 \rightarrow {}^3F_4$, $^3H_5$ spectra, but the IR region was measured with a lower resolution and the satellite structure is difficult to define. Most of the important differences in absorption are connected with $^3H_6 \rightarrow {}^3H_4$, $^3F_3$, $^3F_2$ transitions. To illustrate this, parts of transmission spectra corresponding to $^3H_6 \rightarrow {}^3H_4$ [Fig. 2(a)] and $^3H_6 \rightarrow {}^3F_3$ [Fig. 2(b)] transitions at 100 K are presented. We have chosen for illustration the spectra at 100 K

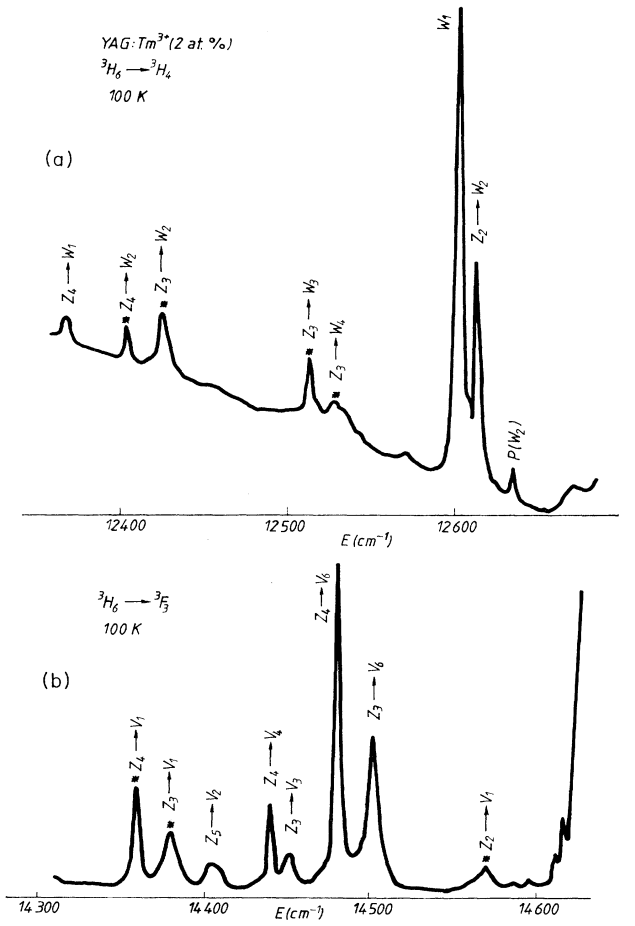

FIG. 2. Part of the transmission spectra of YAG:Tm^{3+} (2 at. %) at 100 K: (a) $^3H_6 \rightarrow {}^3H_4$ transition and (b) $^3H_6 \rightarrow {}^3F_3$ transition.

TABLE II. Part of the $^3H_6 \leftrightarrow {}^3H_4$ Tm^{3+} transmission and luminescence lines in YAG:Tm^{3+} and YAG:Cr^{3+},Tm^{3+} at 77 K. * lines not listed in Ref. 4.

Transmission YAG:Tm^{3+}			Luminescence YAG:Tm^{3+}	YAG:Cr^{3+},Tm^{3+}
E (cm^{-1})	Transition	$\Gamma_i(D_2)$	E (cm^{-1})	E (cm^{-1})
				12 356
12 367	$Z_4 \rightarrow W_1$		12 367	12 367
				12 388
				12 398
*12 406	$Z_4 \rightarrow W_2$		12 406	12 405
*12 428	$Z_3 \rightarrow W_2$		12 428	12 427
*12 515	$Z_3 \rightarrow W_3$		12 516	12 515
*12 532	$Z_3 \rightarrow W_4$		12 532	12 531
				12 583
12 603	$Z_1 \rightarrow P_1(W_1)$			
12 605	M			12 605
12 607	$Z_1 \rightarrow W_1$	Γ_1	12 607	12 608
12 613	$Z_1 \rightarrow P_3(W_1)$		12 613	12 611.5
12 619	$Z_2 \rightarrow W_2$		12618	12 619
12 639	$Z_1 \rightarrow P_1(W_2)$			12 639
12 644	$Z_1 \rightarrow P_2(W_2), W_2$	Γ_2		12 643
12 707				
*12 715	$M(Z_2 \rightarrow W_4)$			
12 721	$Z_2 \rightarrow W_4$			
12 726	$Z_1 \rightarrow P_1(W_3)$			
(12 732)	W_3	Γ_2		
12 735	$Z_1 \rightarrow P_2(W_3)$			
12 741	M			
12 747	$Z_1 \rightarrow W_4$	Γ_3		

since the lines are still sharp but the hot bands are more evident. The lines not reported previously are marked by an asterisk. Experimental lines of part of $^3H_6 \rightarrow {}^3H_4$ absorption and emission spectra in YAG:Tm^{3+} and YAG:Tm^{3+},Cr^{3+} at 77 K are listed in Table II and those of the $^3H_6 \rightarrow {}^3F_3$ transmission spectra are listed in Table III. We kept the notations W_i, V_i for Stark levels and $Z_i \rightarrow W_i$, V_i for hot bands or luminescence lines. In the $^3H_4 \rightarrow {}^3F_2$ region a rather intense but broad line at 15 191 cm^{-1} and a shoulder at 15 184 cm^{-1} were measured at 10 K with a clear hot band structure at 27 cm^{-1} at 77 K. The proposed assignment shall be discussed later.

TABLE III. Transmission spectrum of YAG:Tm^{3+} from $^3H_6$ to $^3F_3$ at 77 K. * lines not listed in Ref. 4.

E			E		
(cm^{-1})	Transition	$\Gamma_i(D_2)$	(cm^{-1})	Transition	$\Gamma_i(D_2)$
*14 360	$Z_4 \rightarrow V_1$		14 665		
*14 383	$Z_3 \rightarrow V_1$		*14 667	$P_1(V_3), V_3$	Γ_2
14 411	$Z_5 \rightarrow V_2$		*14 668	$P_2(V_3)$	
*14 442	$Z_4 \rightarrow V_4$		14 671	$P_1(V_4)$	
14 453	$Z_3 \rightarrow V_3$		14 679	V_4	Γ_4
14 480	$Z_4 \rightarrow V_6$		14 689		
14 502	$Z_3 \rightarrow V_6$		*14 695		
*14 572	$Z_2 \rightarrow V_1$		14 699		
*14 597	$P_1(V_1)$		*14 701	$M(V_5)$	
*14 599	$P_2(V_1), V_1$	Γ_2	14 706	V_5	Γ_3
*14 613			*14 710		
*14 617			14 715	$P_1(V_6)$	
*14 627	$M(Z_2 \rightarrow V_2)$		14 720	V_6	Γ_1
14 632	$Z_2 \rightarrow V_2$		14 724		
14 643	$Z_2 \rightarrow V_3$		*14 728		
14 648			*14 738	$P(Z_2 \rightarrow V_7)$	
14 652	$Z_2 \rightarrow V_4$		14 741	$Z_2 \rightarrow V_7$	
*14 656	$M(V_2)$		14 749		
14 659	V_2	Γ_4	14 770	V_7	Γ_3

Most of the satellite lines in the $^3H_6 \rightarrow {}^3H_4$, $^3H_6 \rightarrow {}^3F_3$ transitions detected in our more concentrated samples were reported by Gruber *et al.*[4] The analysis of the concentration dependence of the satellite structure is difficult, even at 10 K, due to the line broadening. Thus,

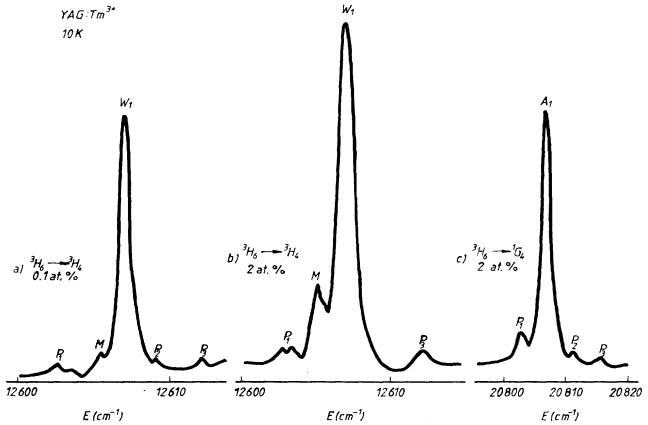

FIG. 3. Satellite structure of Tm^{3+} in YAG at 10 K: (a) and (b) satellites associated with the $Z_1(^3H_6) \rightarrow W_1(^3H_4)$ transition for two concentrations and c satellite structure of $Z_1(^3H_6) \rightarrow A_1(^1G_4)$ transition for 2 at. % Tm^{3+}.

while some of the satellites retain their relative strength at different concentrations, others closer to the main line, seem to exhibit a concentration dependence. A typical example is the satellite structure connected with the $^3H_6(Z_1)\rightarrow{}^3H_4(W_1)$ transmission region, for samples with different Tm^{3+} concentrations [Figs. 3(a) and 3(b)]. Note the small splitting (≈ 0.8 cm^{-1}) of one of the satellites. To demonstrate the complexity of the satellite structure and the necessity of further investigation, we present in Fig. 3(c) one of the sharpest lines in the spectra [$^3H_6(Z_1)\rightarrow{}^1G_4(A_1)$ transition].

Three relatively intense hot bands at 12 406, 12 428, and 12 619 cm^{-1}, observed in the $^3H_6\rightarrow{}^3H_4$ transition [Fig. 2(a), Table II] could not be associated with any Stark component identified previously, or any intense line in our spectra. This suggests that they could be associated with a Stark level at 12 644 cm^{-1} in a region where only small P satellites have been detected. We assume that it corresponds to a forbidden transition from the ground $Z_1(^3H_6)$ level. A similar level is found in the 12 725–12 735-cm^{-1} region. In the $^3H_6\rightarrow{}^3F_3$ transition supplementary hot bands have again been detected and identified with regions where P satellites are present without intense lines. Two Stark levels corresponding to forbidden transitions are proposed: V_1 at 14 599 cm^{-1} and V_3 at 14 667 cm^{-1}. One should mention also that in all these cases the most intense hot band corresponds to the Z_3 (215 cm^{-1}) Stark component of $^3H_6$.

B. YAG:Tm^{3+} luminescence spectra

The Tm^{3+} emission from the $^3H_4$, $^1G_4$, and $^1D_2$ levels has been measured when excited by nonselective pumping with a Xe lamp or third harmonic of a YAG:Nd^{3+} laser

TABLE IV. Energy levels of YAG:Tm^{3+} (cm^{-1}) in D_2 symmetry and proposed symmetry labels.

$^3H_6$	$J=6\rightarrow 4\Gamma_1+3\Gamma_2+3\Gamma_3+3\Gamma_4$
	$Z_1(\Gamma_2)-0$, $Z_2(\Gamma_1)-27$, $Z_3(\Gamma_4)-215$, $Z_4(\Gamma_3)-240$,
	$Z_5(\Gamma_2)-247$, Z_6-300, Z_7-450, Z_8-550, Z_9-590,
	$Z_{10}-607$, $Z_{11}-720$
$^3F_4$	$J=4\rightarrow 3\Gamma_1+2\Gamma_2+2\Gamma_3+2\Gamma_4$
	$Y_1(\Gamma_1)-5\,555$, $Y_2(\Gamma_3)-5\,764$, $Y_3(\Gamma_2)-5\,832$,
	$Y_4(\Gamma_4)-5\,901$, $Y_5(\Gamma_1)-6\,042$, $Y_6(\Gamma_2)-6\,111$,
	$Y_7(\Gamma_1)-6\,143$, $Y_8(\Gamma_4)-6\,170$, $Y_9(\Gamma_3)-6\,199$
$^3H_5$	$J=5\rightarrow 2\Gamma_1+3\Gamma_2+3\Gamma_3+3\Gamma$
	$X_1(\Gamma_2)-8\,257$, $X_2(\Gamma_4)-8\,340$, $X_3(\Gamma_3)-8\,345$,
	$X_4(\Gamma_3)-8\,516$, $X_5(\Gamma_3)-8\,536$, $X_6(\Gamma_4)-8\,556$,
	$X_7(\Gamma_2)-8\,700$, $X_8-8\,787$, $X_9-8\,800$, $X_{10}-8\,833$
$^3H_4$	$J=4\rightarrow 3\Gamma_1+2\Gamma_2+2\Gamma_3+2\Gamma_4$
	$W_1(\Gamma_1)-12\,607$, $W_2(\Gamma_2)-12\,644$, $W_3(\Gamma_2)-12\,732$,
	$W_4(\Gamma_3)-12\,747$, $W_5(\Gamma_4)-12\,823$, $W_6(\Gamma_3)-13\,036$,
	$W_7-13\,078$, $W_8-13\,110$
$^3F_3$	$J=3\rightarrow 1\Gamma_1+2\Gamma_2+2\Gamma_3+2\Gamma_4$
	$V_1(\Gamma_2)-14\,599$, $V_2(\Gamma_4)-14\,659$, $V_3(\Gamma_2)-14\,666$,
	$V_4(\Gamma_4)-14\,679$, $V_5(\Gamma_3)-14\,706$, $V_6(\Gamma_1)-14\,720$,
	$V_7(\Gamma_3)-14\,770$
$^3F_2$	$J=2\rightarrow 2\Gamma_1+\Gamma_2+\Gamma_3+\Gamma_4$
	$U_1(\Gamma_2)-15\,183$, $U_2(\Gamma_4)-15\,190$, $U_3(\Gamma_1)-15\,246$,
	$U_4(\Gamma_3)-15\,263$, $U_5(\Gamma_1)-15\,439$

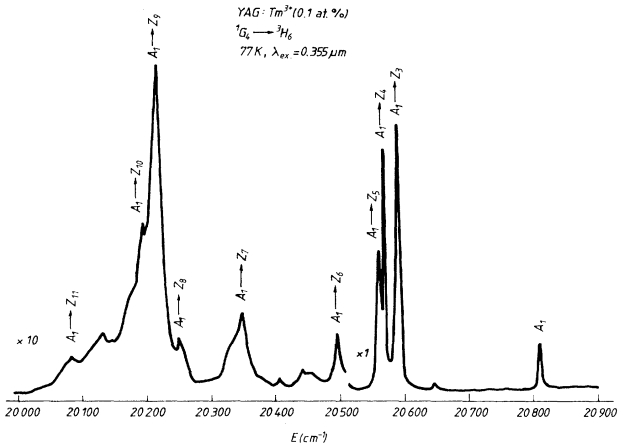

FIG. 4. Luminescence spectra from $^1G_4$ to $^3H_6$ of YAG:Tm^{3+} at 77 K. Part of the spectrum (20 000–20 500 cm^{-1}) is amplified.

(≈ 355 nm, ≈ 10 ns) into a phonon sideband associated with the $^1D_2$ level. Although quenching effects were noticed, our attention was concentrated on the identification of Stark levels for Tm^{3+} multiplets involved in $\approx 2\,\mu$m emission.

The spectra are complicated since, at 77 K, emission from more Stark components can appear. Thus, while the first Stark level of $^1G_4$, A_1(20 808 cm^{-1}), is rather well isolated, at least two levels (W_1 and W_2, Table II) contribute to the emission at 77 K from $^3H_4$. The $^1D_2$ emission shows similar behavior: besides two close Stark components B_1(27 868 cm^{-1}) and B_2 (27 877 cm^{-1}), the emission from other levels can be expected. Our spectra are better resolved and more informative than those previously available.

From the luminescence spectra of $^1D_2$, $^1G_4$, $^3H_4$ to $^3H_6$ ground multiplet, the positions of several $^3H_6$ levels have been identified (Table IV). Most of them are coincident with those obtained from $^3F_4\rightarrow{}^3H_6$ emission.[4] From Fig. 4, where the $^1G_4(A_1)\rightarrow{}^3H_6(Z_i)$ luminescence spec-

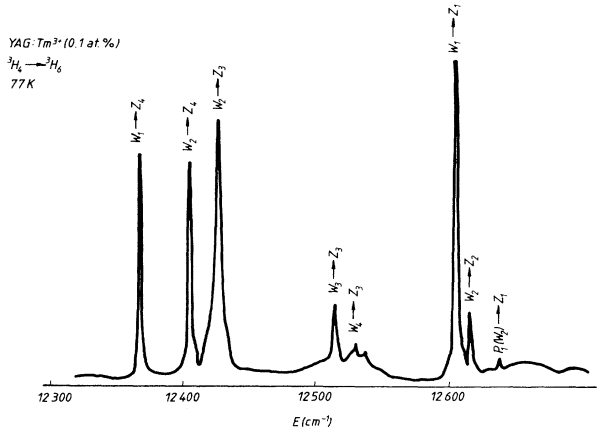

FIG. 5. Part of the $^3H_4\rightarrow{}^3H_6$ emission spectra of a YAG:Tm^{3+} (0.1 at. %) sample obtained at 77 K under nonselective lamp pumping.

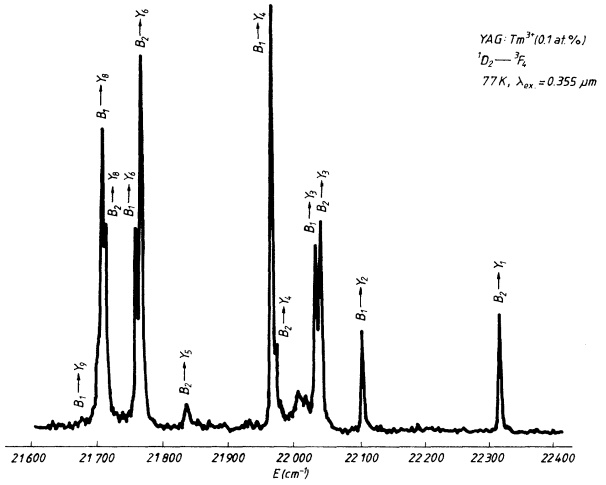

FIG. 6. Luminescence from $^1D_2$ to $^3F_4$ of YAG:Tm^{3+} at 77 K under 0.355-μm laser excitation.

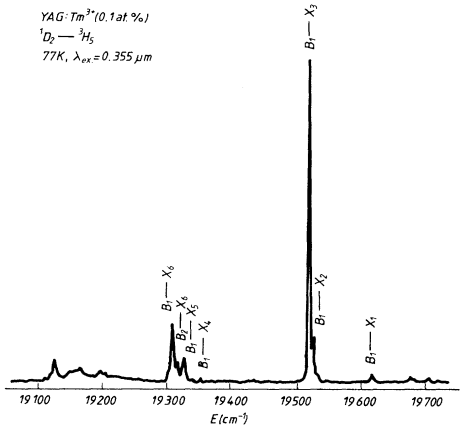

FIG. 7. $^1D_2$ to $^3H_5$ luminescence spectra at 77 K.

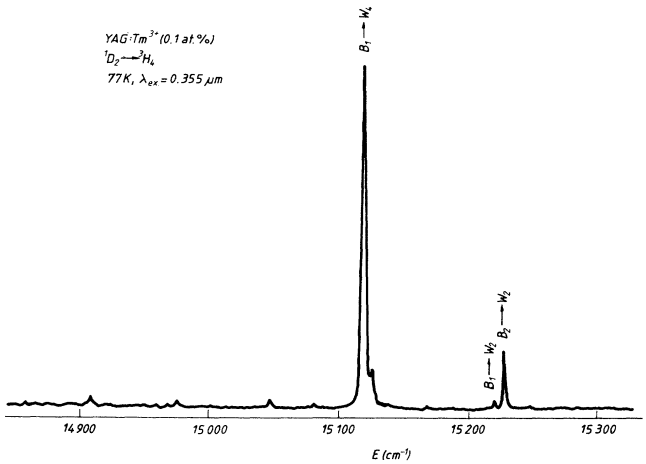

FIG. 8. Luminescence from $^1D_2$ to $^3H_4$ at 77 K.

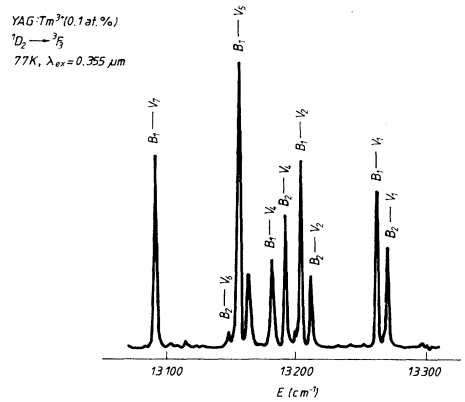

FIG. 9. Luminescence from $^1D_2$ to $^3F_3$ at 77 K.

tra are presented, one can clearly identify the levels Z_3, Z_4, Z_5 observed in absorption. Due to the overlapping of the lines it is difficult to establish the Stark level positions from the amplified region. The emission from $^3H_4$ or $^1D_2$, similarly complicated in these regions, suggests possible Stark levels as given in Table IV.

It is interesting, however, to examine part of the $^3H_4 \rightarrow {}^3H_6$ emission (Fig. 5) excited with a Xe lamp. One can observe a similar structure as in absorption [Fig. 2(a)], which can be explained by the contribution to emission of the least two levels, W_1 and W_2.

The $^1G_4 \rightarrow {}^3F_4$ and $^1D_2 \rightarrow {}^3F_4$ (Fig. 6) luminescence spectra allow verification of a $^3F_4$ level structure as derived from absorption data. Similarly, the $^1G_4 \rightarrow {}^3H_5$ and $^1D_2 \rightarrow {}^3H_5$ (Fig. 7) emissions have been used to verify $^3H_5$ energy levels, $^1D_2 \rightarrow {}^3H_4$ (Fig. 8) for the elucidation of $^3H_4$ multiplet structure, $^1D_2 \rightarrow {}^3F_3$ (Fig. 9) to check the transmission $^3H_6 \rightarrow {}^3F_3$ data and $^1D_2 \rightarrow {}^3F_2$ to identify $^3F_2$ Stark components.

V. YAG:Cr^{3+},Tm^{3+} SPECTRA

A preliminary study has been made of the manner in which double doping with Tm^{3+} and Cr^{3+} affects the transmission spectra. While for low Cr^{3+} and Tm^{3+} content ($\approx$0.1 at. %) the spectra at 77 K look like a superposition of two ion spectra, supplementary satellites are observed at higher concentrations. In the transmission spectra at 77 K an increase of the relative intensity of some satellites with Cr^{3+} content has been noticed. At $\approx$10 K the appearance of new satellite lines is clear. Thus, the transmission spectra of a YAG:Cr^{3+}(0.4%):Tm^{3+}(5%) sample (Fig. 10) shows a clear line broadening in some regions and the appearance of a new peak at 12 611.5 cm^{-1} superimposed on the P_3 satellite at 12 613 cm^{-1}. In the Cr^{3+} $^4A_2 \rightarrow {}^2E$ transition, besides the usual Cr^{3+} lines observed previously in emission, a supplementary satellite Y_1(14 546.5 cm^{-1}) near R_1(14 548 cm^{-1}) has been detected at 77 K. The presence of such a satellite in Cr^{3+} spectra was inferred[8] from the $^3H_4$ Tm^{3+} excitation spectra in YAG:Cr^{3+}, Tm^{3+}, Ho^{3+} and as-

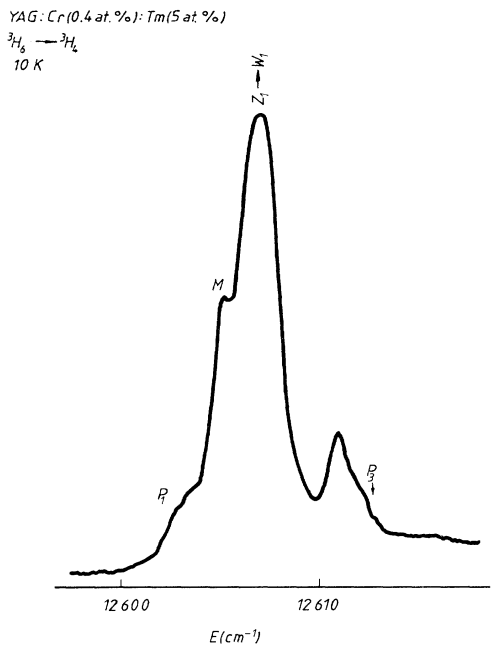

FIG. 10. The satellite structure associated with $Z_1(^3H_6) \rightarrow W_2(^3H_4)$ transmission spectra for a YAG:Cr^{3+} (0.4 at. %):Tm^{3+} (5 at. %) sample.

signed to a Cr^{3+} site due to the presence of Tm^{3+} in its proximity.

The Tm^{3+} emission in the $^3H_4 \rightarrow {}^3H_6$ region, in doubly doped samples under lamp or laser (0.532 μm) pumping, was also measured at 77 K. The spectra are more complex than for single doped samples. For example, part of the $^3H_4 \rightarrow {}^3H_6$ luminescence spectra of a YAG: Cr^{3+}(0.4%):Tm^{3+}(5%) samples is presented in Fig. 11. The emission seems to come from the activation of some Tm^{3+} satellites in Cr^{3+}-codoped samples. Table II presents a comparison of the luminescence emission lines

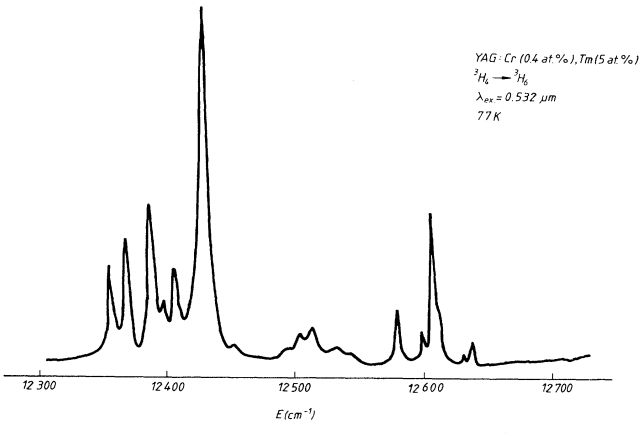

FIG. 11. Part of the $^3H_4 \rightarrow {}^3H_6$ luminescence spectra of YAG:Cr^{3+} (0.4 at. %):Tm^{3+} (5 at. %) at 77 K under 0.532-μm laser excitation.

in YAG:Tm^{3+} and YAG:Tm^{3+},Cr^{3+} at 77 K. The subsequent investigation by site-selective excitation, at low temperatures has shown that in codoped samples the Tm^{3+} emission is dominated by three new centers[14,15] their energy levels being slightly shifted from W_1 (12 607) cm^{-1}), i.e., at 12 605, 12 608, and 12 611.5 cm^{-1}.

VI. DISCUSSION

This section presents an interpretation of our unpolarized spectral data. First, the energy levels for the lowest multiplets of Tm^{3+} (c) in D_2 sites in YAG shall be discussed. To assign symmetry labels to the Stark components we have adopted, with some improvement, the algorithm used previously.[4] Assuming that the symmetry of the ground $^3H_6$ Stark component is Γ_2, the identification of excited Γ_1 levels is based on the lack of a hot band at Z_2 (27 cm^{-1}), as the absorption to the $^3P_0$ (Γ_1) level shows, and the possibility of transitions from/to Z_3, Z_4 and Z_5 Stark levels; Z_2 is a Γ_1-type level.

In the assignment of Γ_2 excited levels we propose to use the spectra connected with minority sites. Thus, for such sites (with C_s or C_1 symmetry) leading to P satellites, the distortion of D_2 is rather strong and relatively intense lines could correspond to $\Gamma_i \rightarrow \Gamma_i$ forbidden transitions in D_2. Excited Γ_2 levels could be identified in regions where P satellites are present without noticeable absorption lines. Our data (on $^3H_4$, $^3F_3$) suggest that the most probable transitions associated with Γ_2 levels are at Z_3 (215 cm^{-1}). Transitions from and to $Z_2(\Gamma_1)$ are also expected. The symmetry of Z_3 could be assigned by convention, similar to that used in polarization measurements of YAG:Tb^{3+}.[10] Since local symmetry D_2 at Tm^{3+} (c) is a slight distortion of D_{2d}, the $\Gamma_2 \leftrightarrow \Gamma_4$ transitions in D_2 are compatible with an electric dipole-allowed transition in D_{2d} ($\Gamma_5 \rightarrow \Gamma_5$). One can, by convention, assume that $\Gamma_2 \leftrightarrow Z_3$ intense lines correspond to $\Gamma_2 \leftrightarrow \Gamma_4$ allowed transitions. This establishes Z_3 as a Γ_4 level. The luminescence data confirm our identification of Γ_2 levels based on these arguments.

As observed earlier, by analyzing our spectra, we found that hot bands from Stark levels Z_2, Z_3, and Z_5 or Z_2, Z_4, and Z_5 have Γ_3 or Γ_4 symmetry. The distinction can be made if the symmetry of Z_3 and Z_4 is known. Using the above data concerning the possible symmetry of Z_3, as well as luminescence spectra, we can associate Z_3 with Γ_4, Z_4 with Γ_3, and Z_5 with Γ_2 symmetries. Thus, the ideal hot band structure for Γ_3 levels is Z_2, Z_3, and Z_5, while for Γ_4 it is Z_2, Z_4, and Z_5. In many cases the identification is difficult due to the overlap or low intensities of some lines.

Using this algorithm and our spectral data, a series of Stark levels of $^3H_6$, $^3F_4$, $^3H_5$, $^3H_4$, $^3F_3$, and $^3F_2$ multiplets have been identified (Table IV). For the interpretation of luminescence spectra higher levels have also been investigated. The symmetry of the $A_1(^1G_4)$ Stark level is Γ_1 (Fig. 4), while the assignment of the two lowest components of $^1D_2$ as B_1-Γ_1 and B_2-Γ_3 is in agreement with Ref. 4. Thus, in the $^1D_2$ luminescence one could expect to have either singlets if the terminal level has Γ_1 or Γ_3

symmetry or doublets separated by 8–10 cm^{-1} (B_1-B_2) if the terminal level has Γ_2 or Γ_4 symmetry. Contribution from higher levels of $^1D_2$ (situated with ≈ 150 cm^{-1} above B_1) is also possible.

To the $^3H_6$ multiplet energy level scheme we could not achieve any improvement, although the $^3H_4$, $^1G_4$, and $^1D_2$ emission was carefully analyzed. Besides the Z_1-Z_5 levels also observed in absorption, most of the other intense peaks have also been detected in $^3F_4 \rightarrow {}^3H_6$ luminescence.[4] Other Stark levels are possible at ≈ 300 cm^{-1} or in the 650–690-cm^{-1} region.

In the energy level assignments of the $^3F_4$ multiplet we propose several changes based especially on luminescence data. The lack of any emission from $A_1(^1G_4)$ or B_1, $B_2(^1D_2)$ to the Y_2(5732 cm^{-1}) Stark level observed in our absorption spectra as an intense line, and the presence of a strong luminescence at 22 102 cm^{-1} in $^1D_2 \rightarrow {}^3F_4$ (Fig. 6) emission lead us to identify the Y_2 Stark level at 5764 cm^{-1} (where a small absorption line is detected) as a Γ_3 type with an intense $Z_2 \rightarrow Y_2$ hot band at 5732 cm^{-1}. The luminescence line at 22 106 cm^{-1} would correspond to a $B_1 \rightarrow Y_2$ ($\Gamma_1 \rightarrow \Gamma_3$) transition. The luminescence data and hot bands (less clear in the IR region) also suggest that the Y_3 level (6170 cm^{-1}) could be of Γ_4 type. The strong absorption at 6143 cm^{-1} (also observed in Ref. 4) exhibits a slight temperature dependence and could be a superposition of a Stark component Y_7 and a $Z_2 \rightarrow Y_8$ hot band. Our spectra also suggest a possible level Y_9 at 6199 cm^{-1}, but the assignments of the latter two levels is less certain.

We could not completely identify all the Stark components of the $^3H_5$ multiplet (Table IV). The spectra are less intense and overlapping and the luminescence from $^1G_4 \rightarrow {}^3H_5$ is superimposed on the emission from $^1D_2 \rightarrow {}^3F_2$ (Table IV). Nevertheless, we propose several changes from data given in Ref. 4. To explain a rather strong hot band in absorption at 8042 cm^{-1} and two luminescence lines (19 616 and 19 622 cm^{-1}) in the $^1D_2 \rightarrow {}^3H_5$ (Fig. 7) spectra we assume the presence of a Γ_2-type Stark level at ≈ 8257 cm^{-1} (X_1). From $^1G_4$, $^1D_2 \rightarrow {}^3H_5$ luminescence a possible Stark level of Γ_3 symmetry (X_5) is assumed around 8536 cm^{-1}. The spectral region corresponding to 8700–8800 cm^{-1} is unclear in absorption and luminescence as well.

The elucidation of $^3H_4$ Stark structure at high energies (12 830–13 200 cm^{-1}) is difficult due to overlapping of the transitions between Stark levels with phonon side bands and hot bands. Besides, $^1D_2 \rightarrow {}^3H_4$ (Fig. 8) emission is superimposed on $^1G_4 \rightarrow {}^3F_4$ spectra and only a part of the spectra could be assigned. As discussed before, $^3H_4 \rightarrow {}^3H_6$ spectra at 77 K [Fig. 2(a), Fig. 5, Table II] could be explained by assuming the presence of two Γ_2 levels, W_2 (12 644 cm^{-1}) and W_3 (12 730 cm^{-1}) in regions where only small satellites are observed in absorption. $^1D_2 \rightarrow {}^3H_4$ (Fig. 8) clearly confirm the existence of W_2 and W_3 levels. Our measurements also suggest that the intense absorption line 12 747 cm^{-1} (W_4) most likely has Γ_3 symmetry and W_5 at 12 823 cm^{-1} could be a Γ_4-type level.

In Table III, the position of absorption lines connected with a $^3H_6 \rightarrow {}^3F_3$ transition is given, the symmetry assignments also being verified with the help of $^1D_2 \rightarrow {}^3F_3$ (Fig. 9) luminescence spectra. One must stress that the luminescence clearly verifies the presence of a Γ_2 level V_1, with a less sure identification of V_3. This could be an important point since, in our assignment, the lowest Stark level of $^3F_3$ is situated ≈ 60 cm^{-1} below the previous proposal and in a region where, at low temperatures, ^2E (Cr^{3+})-$^3F_3$(Tm^{3+}) energy transfer can take place. Another peculiarity of the emission spectra to $^3F_3$ is that no clear luminescence line can be associated with relatively intense absorption line at 14 741 cm^{-1}, while there is a clear singlet line at 13 090 cm^{-1} that could be associated with a $B_1(^1D_2)$ transition to a less intense absorption line at 14 770 cm^{-1} (also observed in Ref. 4). Thus, one can assume that the highest Stark level of $^3F_3$ is V_7 at 14 770 cm^{-1}, has Γ_3 symmetry, and the 14 741-cm^{-1} line is a $Z_2 \rightarrow V_7$ hot band corresponding to a $\Gamma_1 \rightarrow \Gamma_3$ transition.

In the assignment of the Stark structure of the $^3F_2$ multiplet we propose several changes, based on our absorption data at 10 K and higher temperatures and the $^1D_2 \rightarrow {}^3F_2$ emission data. The supplementary line at 15 191 cm^{-1} and its shoulder at 15 184 cm^{-1} are assigned to Stark levels with the symmetry identification as given in Table IV.

From analysis of the spectra we observe that the lines associated with $\Gamma_2 \leftrightarrow \Gamma_4$ transitions (P_Z type) are relatively intense while some of the lines that could be associated with $\Gamma_1 \leftrightarrow \Gamma_3$-($P_Z$) transitions have very low intensity. Similar arguments as used for Pr^{3+} in YLF (Ref. 9) can explain these points.

The satellite structure of Tm^{3+} in YAG is unlikely to be connected with unwanted impurities, since most of lines are also reported in Ref. 4. This structure is similar to that observed for other rare-earth ions in garnets. The P satellites have a relative intensity, independent of concentration, of 2–3 % (as determined from transmission spectra) and could be assigned to a Tm^{3+} (c) close to a Y^{3+} (a) nonstoichiometric defect. P satellites have been resolved near most of the $^3H_6 \rightarrow {}^3H_4$, $^3F_3$ lines, with shifts from the main lines up to ≈ 15 cm^{-1}. Selective excitation and low-temperature measurements are necessary to elucidate the satellite structure.

Preliminary analysis of double doped samples has revealed changes in both the Tm^{3+} and Cr^{3+} spectra. In the supplementary lines seen in the Tm^{3+} transmission spectra, an apparent intensity increase and broadening of some satellites was observed in Cr^{3+}-codoped samples. These effects could be associated with Tm^{3+} (c)-Cr^{3+} (a) "pairs" spectrally situated close to the Tm^{3+} satellite lines. Some supplementary shoulders in Cr^{3+} spectra were also noticed. The $^3H_4 \rightarrow {}^3H_6$ luminescence spectra at 77 K of the doubly doped samples (Fig. 10) is more complex than for singly doped ones. Thus, in Table II part of the $^3H_4 \rightarrow {}^3H_6$ luminescence lines at 77 K in singly doped and Cr^{3+}-codoped YAG:Tm^{3+} are given. If for YAG:Tm^{3+} the spectrum is dominated by the normal (D_2) center emission, for YAG:Cr^{3+}:Tm^{3+} different centers dominate the spectrum, even under nonselective

excitation. There are three such centers, as the site-selective measurements have confirmed,[14,15] that could be associated with Cr^{3+} (*a*)-Tm^{3+} (*c*) near-neighbor "pairs," in accord with structure data. For such sites having a lower symmetry, all the transitions are allowed, so the structure of the spectra is more complex. Thus, besides the previously discussed $\Gamma_2 \rightarrow \Gamma_2$ transitions, luminescence lines corresponding to former $(D_2)\Gamma_1 \rightarrow \Gamma_1$ forbidden transitions could be assigned. For instance, a clear luminescence line at 12 584 cm^{-1} can be associated with a transition from a satellite (12 611.5 cm^{-1}) close to the $W_1(\Gamma_1)$ level, to the $Z_2(\Gamma_1)$.

One must stress that all the entities discussed above have their own energy level diagrams and could be selectively excited. Energy transfer processes dependent on temperature and concentration could take place between these entities and modify the luminescence relative intensities and luminescence decays. The presence of a multisite structure is expected to influence even the global luminescence decays leading to excitation and detection wavelength dependences. In the analysis of Tm^{3+} luminescence kinetics one can expect quenching rates for the Tm^{3+}-Tm^{3+} or Cr^{3+}-Tm^{3+} near-neighbor pairs that are different from those between more distant ions. Such research is now in progress.

In conclusion, from the analysis of absorption and emission spectra of Tm^{3+} in YAG and Cr^{3+}-codoped YAG:Tm^{3+}, we have been able to identify new levels of Tm^{3+} in the normal D_2 sites, especially in the $^3H_4$, $^3F_3$, $^3F_2$ levels involved in the $\approx$2-μm laser emission. We have established Γ_2 levels in the $^3H_4$ multiplet that can explain the luminescence data and in $^3F_3$ that could be important for Cr^{3+}-Tm^{3+} energy transfer. The Tm^{3+} emission lines in Cr^{3+}-codoped samples, probably due to Tm^{3+} (*c*)-Cr^{3+} (*a*) pairs, could be explained by a preferential energy transfer.

ACKNOWLEDGMENTS

The authors wish to thank Dr. S. Georgescu for help in experiments and M. Bolog and his group for growing the samples.

[1]G. S. Quarles, A. Rosenbaum, C. L. Marquardt, and L. Esterowitz, Opt. Lett. **15**, 42 (1990).
[2]T. Becker, G. Huber, H. J. v. d. Heide, P. Mitzcherlich, B. Struve, and E. W. Duczynski, Opt. Commun. **80**, 47 (1990).
[3]T. Becker and G. Huber, J. Phys. (Paris) Colloq. **52**, C7-353 (1991).
[4]J. B. Gruber, M. E. Hills, R. C. Macfarlane, C. A. Morrison, G. A. Turner, C. J. Quarles, C. J. Kintz, and L. Esterowitz, Phys. Rev. B **40**, 9464 (1989).
[5]G. M. Zverev, G. Ya. Kolodnyi, and A. M. Onishchenko, Zh. Eksp. Teor. Fiz. **57**, 754 (1989).
[6]B. M. Antipenko and Yu. V. Tomashevich, Opt. Spectrosc. **44**, 272 (1978).
[7]W. Nie, G. Boulon, and J. Mares, Chem. Phys. Lett. **160**, 597 (1989).
[8]W. Nie, Y. Kalinsky, C. Pedrini, A. Monteil, and G. Boulon, Opt. Quantum Electron. **22**, AS123 (1990).
[9]L. Esterowitz, F. J. Bartoli, and R. E. Allen, J. Lumin. **21**, 1 (1979).
[10]R. Bayerer, J. Heber, and D. Mateika, Z. Phys. B **64**, 201 (1986).
[11]F. Euler and J. A. Bruce, Acta Crystallogr. **19**, 971 (1965).
[12]Yu. K. Voronkov and A. A. Sobol, Phys. Status Solidi **27**, 257 (1975).
[13]N. Y. Agladze, H. S. Bagdasarov, E. A. Vinogradov, V. I. Zhekov, T. M. Murina, N. N. Popova, and E. A. Fedov, Kristallografia **33**, 913 (1988).
[14]A. Lupei, C. Tiseanu, V. Lupei, and S. Georgescu, in Proceedings of the International Conference on Defects in Insulating Materials, Nordkirchen, Germany, 1992 (in press).
[15]V. Lupei, L. Lou, G. Boulon, A. Lupei, and C. Tiseanu, J. Phys. (Paris) (to be published).